

Slowing hot-carrier relaxation in graphene using a magnetic fieldP. Plochocka,^{1,*} P. Kossacki,^{1,2} A. Golnik,² T. Kazimierczuk,² C. Berger,³ W. A. de Heer,³ and M. Potemski¹¹*Laboratoire National des Champs Magnétiques Intenses, Grenoble High Magnetic Field Laboratory, CNRS, 25 Avenue des Martyrs, 38042 Grenoble, France*²*Institute of Experimental Physics, University of Warsaw, Warsaw, Poland 30328*³*Georgia Institute of Technology, Atlanta, Georgia, USA*

(Received 1 October 2009; revised manuscript received 5 November 2009; published 10 December 2009)

A degenerate pump-probe technique is used to investigate the nonequilibrium carrier dynamics in multi-layer graphene. Two distinctly different dynamics of the carrier relaxation are observed. A fast relaxation (~ 50 fs) of the carriers after the initial effect of phase-space filling followed by a slower relaxation (~ 4 ps) due to thermalization. Both relaxation processes are less efficient when a magnetic field is applied at low temperatures which is attributed to the suppression of the electron-electron Auger scattering due to the nonequidistant Landau-level spacing of the Dirac fermions in graphene.

DOI: [10.1103/PhysRevB.80.245415](https://doi.org/10.1103/PhysRevB.80.245415)

PACS number(s): 78.66.Tr, 78.20.Ls, 78.47.J-, 78.67.Pt

I. INTRODUCTION

Carrier scattering due to the Coulomb interaction is usually regarded as the dominant process which governs the dynamics of hot carriers in solids at very short time scales.¹ This is true for conventional (semiconductor) two-dimensional systems, even when their energy bands are quantized into discrete Landau levels by the application of a magnetic field. This is because Auger-type scattering processes between equidistant Landau levels, formed from bands with parabolic dispersions, are extremely efficient.² Indeed, Auger scattering has long been considered as the main obstacle for the fabrication of tunable far-infrared laser based on inter-Landau-level emission.³ For example, hot carriers generated by a strong electrical field give rise only to weak cyclotron emission.^{4,5} However, the application of a magnetic field should considerably influence the electron-electron scattering process in strongly nonparabolic electronic systems.

Graphene, a single monolayer of hexagonally arranged carbon atoms, is a two-dimensional system with quite unique electronic properties mostly related to its peculiar band structure.⁶⁻⁹ In particular, carriers at the K and K' points of the Brillouin zone, where the conduction and valence bands touch, have a linear dispersion relation and therefore behave as massless Dirac particles. A direct consequence of the linear dispersion is the rather unusual Landau quantization, $E_n = \pm \tilde{c} \sqrt{2e\hbar B |n|}$, where $\tilde{c} \approx 10^6$ m/s is the effective speed of light (Fermi velocity) in graphene. Thus, in graphene the Landau levels follow a square-root dependence with the magnetic field and are not equally spaced. Electron-electron scattering (Auger processes) should therefore be strongly suppressed in magnetic field creating favorable conditions for cyclotron emission and population inversion.¹⁰ A first step in this direction would be to demonstrate the suppression of Auger processes for carriers in graphene in a magnetic field. Previous ultrafast spectroscopic investigations¹¹⁻¹⁴ show that the electron-electron scattering occurs on the time scale of a few tens of femtoseconds in the absence of an external magnetic field. The influence of the Landau quantization on electron-electron scattering has so

far not been investigated to the best of our knowledge.

In this paper we investigate the dynamics of the nonequilibrium carriers in graphene measured using a degenerate pump-probe technique which directly probes the occupancy of states well above the Fermi level. Two characteristic relaxation times are observed. A fast process (~ 50 fs) which broadens the photocreated distribution and a slower process (~ 4 ps) due to thermalization. Applying an external magnetic field leads to a significantly longer relaxation for both processes. This is attributed to a reduction in the electron-electron scattering due to energy conservation, e.g., Auger scattering is blocked due to the nonequidistant Landau-level spacing in graphene. The similar behavior suggests that electron-electron (Auger) scattering plays an important role in both the fast and slow relaxation processes.

II. EXPERIMENT

The experiment was performed in the pump-probe configuration using a Ti:Sapphire mode-locked laser. The repetition rate was 80 MHz, pulse width ~ 50 fs, central wavelength around 800 nm (1.6 eV), and spectral width ≈ 35 nm. Most of the measurements have been performed using a pulse energy of approximately 1.7 nJ corresponding to the maximum pump-pulse power of 140 mW. The pump and probe pulses had the same wavelength and were colinearly polarized. Both beams were focused at the same place on the sample with a spot size of ~ 200 μm and an angle between pump and probe beams smaller than 10° . The two beams were individually chopped with different frequencies f_1 and f_2 close to 2 kHz. The change in the intensity of the probe pulse (differential transmission), at different delays between the pump and probe pulses, was measured using phase-sensitive detection at the sum frequency ($f_1 + f_2$). The magnetic field was applied in the Faraday configuration, perpendicular to the decoupled graphene layers. The numbers of carriers created by the pump pulse can be estimated for the maximum power of the pump pulse. Using the accepted value of 2.5% for the absorption of a single graphene layer, the number of photocreated carriers per layer is of the order of 10^8 , corresponding to a carrier density of

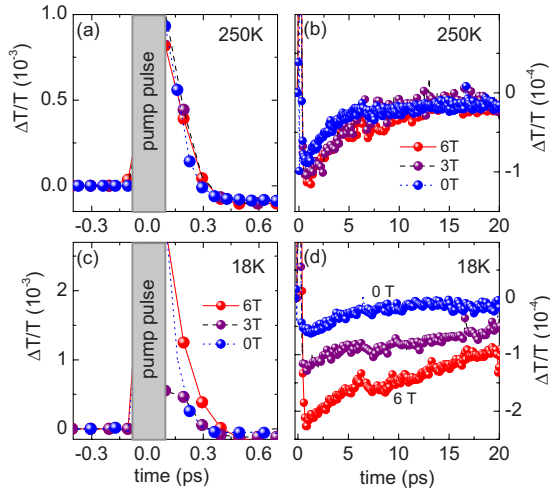


FIG. 1. (Color online) The differential transmission $\Delta T/T$ as a function of the delay between the pump and probe pulses measured at a temperature of [(a)–(b)] 250 K and [(c)–(d)] 18 K for magnetic fields in the range 0–6 T.

$\sim 3 \times 10^{11} \text{ cm}^{-2}$. The investigated samples contain a high number of graphene layers (between 70 and 100) grown in vacuum in an induction heating furnace by the thermal decomposition method, on a (4H) SiC substrate.^{15,16} Experimental data confirm that the investigated layers exhibit the Dirac-type electronic spectrum so that the system can be considered as a multilayer graphene sample.^{16–19}

III. RESULTS AND DISCUSSION

A. Enhanced transmission and phase-space filling

The differential transmission $\Delta T/T$ as a function of delay between the pump and probe pulses, measured at $T = 250 \text{ K}$, is presented in Figs. 1(a) and 1(b) for magnetic fields in the range 0–6 T. For negative delays (before the pump pulse) the differential transmission $\Delta T/T$ is equal to zero. At zero delay [Fig. 1(a)], $\Delta T/T$ increases significantly indicating that the sample becomes more transparent under the influence of the pump pulse. Immediately after the pump pulse, a fast decrease in the signal is observed which is direct evidence that the absorption increases. Interestingly, for delays longer than $\sim 300 \text{ fs}$ the differential transmission changes sign becoming negative. Thus, under the influence of the pump pulse the absorption of the sample is larger than if there was no perturbation at all. Subsequently, the negative signal decays with a characteristic time scale of the order of a few picoseconds, much longer than the time scale of the initial decay [see Fig. 1(b)]. It is clear from the data that at high temperature (250 K) the magnetic field has almost no influence on the carrier relaxation.

The observed increase in the differential transmission under the influence of the pump pulse can be explained using a simple phase-space (Pauli) blocking argument.^{11–14} The pump pulse creates a hot electron-hole plasma with an approximately Gaussian distribution of carriers centered at $\pm 800 \text{ meV}$ and with a width $\approx 100 \text{ meV}$. In our degenerate measurements the pump and probe pulses have the same

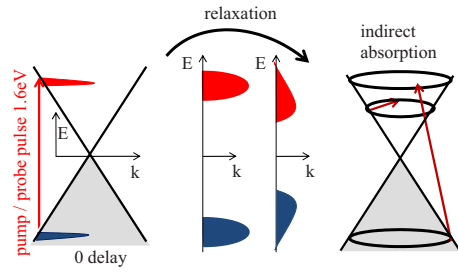


FIG. 2. (Color online) Schematic illustration of the indirect absorption process (relaxed conservation of momentum) for the electron-hole pair created by the probe pulse in the presence of a hot-carrier distribution. The photo-created distribution broadens and finally becomes asymmetric as the system cools. In the presence of the broad hot-carrier distribution indirect transitions involving the simultaneous scattering of an electron at a different energy are allowed. As discussed in the text, relaxation involves both electron-electron and electron-phonon scatterings.

wavelength so that the absorption of the probe pulse at the same delay will decrease due to a blocking (filling) of the available states by the carriers created by the pump pulse. At the energy of the pump pulse in the conduction band the number of available states over the width of the pump pulse is of the order of 10^{13} cm^{-2} . This means that even at the maximum pump-pulse power used only a few percent of the available phase space at this energy is filled. Measurements at higher power show that the increase in the differential transmission varies linearly with power¹¹ and the value of $\Delta T/T$ measured in our experiment agrees with the data in Refs. 11–14 for similar excitation powers.

$\Delta T/T$ then decays quickly due to electron-electron scattering in which the photo-created carrier distribution rapidly broadens as pairs of electrons scatter to lower and higher energy. The reduced phase-space filling makes the sample less and less opaque for the probe pulse. Our results are also in agreement with the findings of similar measurements.^{11,14} The characteristic decay time obtained by fitting an exponential decay to this part of the data is of the order of 70 fs, which is close to the temporal resolution of our experiment.

B. Enhanced absorption and many-body effects

After the decay of the initial increase in transmission, the subsequent increase in the absorption (negative $\Delta T/T$) can be attributed to indirect absorption involving interaction with the now broad distribution of photo-created carriers (many-body processes). It can be described as a scattering which allows transitions with relaxed conservation of the momentum \vec{k} of the electron-hole pair created by the probe pulse, which is illustrated schematically in Fig. 2. In contrast to the phase-space filling, which arises due to the population of photo-created electrons at the same energy as the pump excitation, indirect absorption involves scattering with electrons at different energies. The two processes compete, with phase-space filling dominating at very short delays. However, once the photo-created distribution broadens and decays in energy, phase-space filling is reduced while many-body processes involving scattering with electrons at different en-

ergies remain possible. After a certain delay the carriers form a hot Fermi-Dirac distribution, however our experiment is not sensitive to the particular shape of the carrier distribution. Experiments using a probe pulse in the terahertz (THz) regime¹⁴ suggest that a hot Fermi-Dirac distribution is formed around 150 fs after the pump pulse. One can think that at longer delays the many-body processes increase the available phase space for absorption at the pump/probe energy through non- \vec{k} conserving photon absorption. It is well established that similar scattering processes at the Fermi level lead to the enhancement of the absorption and the appearance of the so-called Fermi edge singularity.²⁰ In our case, the probe pulse excites electrons high in the Dirac cone well above the Fermi level. A similar enhanced absorption was recently observed in both graphene²¹ and graphite²² and described in terms of a modification of the electronic levels by the population of the photo-created carriers. It seems likely that many different scattering processes are possible, even those including more than two carriers. The scattering process presented in Fig. 2 seems to be the most probable due to the temporal evolution (cooling) of the distribution of the carriers but it should be treated only as a schematic representation.

Thus, it seems likely that the same scattering mechanism based on electron-electron interaction leads to the enhancement of the absorption observed in our experimental data. The enhanced absorption decays with a characteristic time of a few picoseconds due to carrier thermalization via intraband carrier scattering (also Auger scattering) and by interband recombination of the photo-created carriers. In our experiment we are unable to distinguish between these processes as we do not probe the occupation close to the Dirac point. Measurements with a THz wavelength probe pulse¹⁴ suggest that first there is a rather fast cooling of the broad distribution of carriers with interband phonons or cold carriers present in the sample on a time scale of 0.15–1 ps leading to the thermalization of the carriers which is followed by electron-hole recombination on the time scale of the order of a few picoseconds.

C. Carrier relaxation in a magnetic field

We turn now our attention to the influence of the magnetic field on the carrier dynamics. In Figs. 1(c) and 1(d) is plotted $\Delta T/T$ versus delay time measured at a temperature of 18 K for magnetic fields in the range 0–6 T. The magnetic field has a considerable influence on both the fast relaxation [Fig. 1(c)] and the slow relaxation [Fig. 1(d)]. For the latter, magnetic field greatly increases the amplitude of the negative differential transmission while at the same time slowing down the thermalization. This can be seen more clearly in Fig. 3 which plots $\ln(\Delta T/T)$ versus delay time to highlight the exponential character of the relaxation. The characteristic time of the decay (τ_r) can be extracted from the slope of such a plot. For the slow relaxation [Fig. 3(b)] at zero magnetic field there is little difference between the high- and low-temperature data with a relaxation time of $\tau_r \sim 4$ ps at both 18 and 250 K. The relaxation becomes slower by a factor of 3–4, changing from $\tau_r \sim 4$ ps at $B=0$ T to $\tau_r \sim 12$ –14 ps

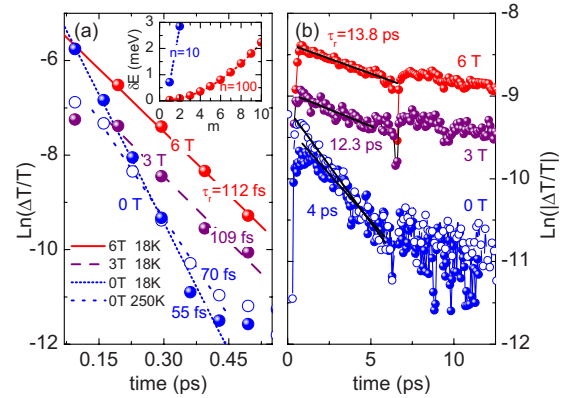


FIG. 3. (Color online) [(a)–(b)] Natural log of the differential transmission as a function of a delay between pump and probe pulses measured for magnetic fields (0–6 T) at 18 K. The $B=0$ T data measured at 250 K is plotted using open circles. The relaxation times τ_r extracted from linear fits are indicated. The inset of (a) shows the calculated energy mismatch [Eq. (1)] for Auger processes for carriers in the $n=10$ and $n=100$ Landau level versus change in Landau-level index m .

for magnetic fields above 3 T. The fast decay of $\ln(\Delta T/T)$ at low temperatures is plotted in Fig. 3(a) for different magnetic fields. Data measured at zero magnetic field and 250 K is also shown for comparison. Without magnetic field there is little difference between the high- and low-temperature data with a relaxation time of $\tau_r \sim 55$ fs at 18 K and $\tau_r \sim 70$ fs at 250 K. However, at low temperatures, the application of a modest magnetic field ~ 3 –6 T doubles the relaxation time to $\tau_r \sim 110$ fs, providing direct experimental evidence that the electron-electron scattering is significantly less effective in the presence of Landau quantization. This slow down, which is common for both the slow and fast relaxation processes, can be seen as a proof that in both cases the electron-electron scattering or thermalization of the hot plasma with the cold electrons is reduced in the presence of Landau quantization which limits the possible energy of the initial and final states.

This is in contrast to standard two-dimensional electron-gas systems in which Auger scattering is enhanced^{2,23} when the zero magnetic field density of states collapses onto equally spaced Landau levels, increasing both the initial and final density of states. In such an Auger process two electrons in Landau level n , scatter, respectively, to the $n+m$ and $n-m$ Landau levels ($m=1,2,\dots$) conserving total energy. Processes involving the scattering of two electrons from Landau level n , to Landau levels $n+m$ and $n-q$ with $m \neq q$, are forbidden due to quasiangular momentum (k -vector) conservation. It has been shown theoretically²⁴ that the most efficient scattering is to the adjacent Landau levels ($m=1$). The total probability of scattering to the outlying Landau levels ($m=2,3,4,\dots$) is roughly the same as the probability of scattering to the nearest Landau level ($m=1$). The authors also show that the higher the Landau-level index the larger the probability of the scattering with a change in the index $m > 1$. In principle, the nonequidistant energetic separation of the Landau levels in graphene is expected to suppress Auger scattering since energy conservation is not fulfilled.

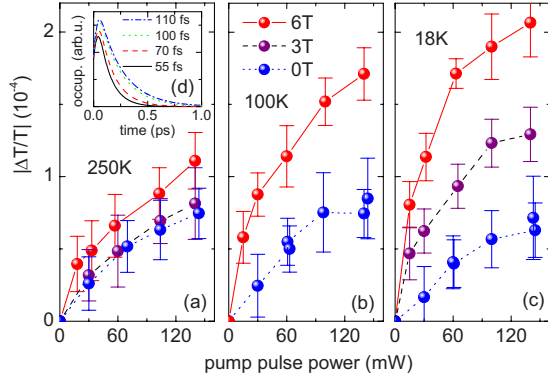


FIG. 4. (Color online) [(a)–(c)] Pump-probe power dependence of $|\Delta T/T|$ for a positive delay corresponding to the maximum enhanced absorption (negative $\Delta T/T$) measured at different temperatures for magnetic fields (0–6 T). (d) Results of a simple rate-equation model; the calculated occupation of the state assuming different lifetimes (relaxation rates) and a Gaussian temporal shape for the generation function.

An enhancement of the cyclotron emission has been reported in *p*-type Germanium due to nonequidistant light-hole Landau levels separation, however the situation is complicated due to the light hole-heavy hole mixing.²⁵ In graphene, the energy mismatch for Auger processes between Landau levels is

$$\delta E = \tilde{c}\sqrt{2e\hbar B}(2\sqrt{n} - \sqrt{n+m} - \sqrt{n-m}) \quad (1)$$

with $n \approx 100$ for the absorption of 1.6 eV radiation at $B = 6$ T. The energy mismatch versus m is plotted in the inset of Fig. 3(a). The Landau-level spacing is a few meV at this energy and this magnetic field, comparable to the Landau-level broadening²⁶ so that the density of states is expected to be modulated even though discrete Landau levels are almost certainly not resolved. Under such conditions Auger scattering should not be significantly suppressed at least for $m=1$. However, with increasing m , the energy difference increases reducing the overlap in phase space for Auger scattering. Thus, under the experimental conditions employed we observe a reduction in the scattering time of only around a factor of 2. Exciting at lower energies (lower n), where the separation between Landau levels is larger, should lead to a considerably more efficient blocking of Auger scattering, as can be seen in Fig. 3(a) where we also plot the expected energy mismatch for $n=10$. Further pump-probe measurements at THz frequencies are planned to verify this hypothesis. The reduction in Auger scattering under magnetic field reported here is an important observation since it potentially opens the way for cyclotron emission or even lasing in graphene.

D. Power dependence of enhanced absorption

Finally, to verify the hypothesis that the enhanced absorption (negative $\Delta T/T$) is related with scattering with photo-created electrons we have investigated this effect as a function of the power of the pump pulse, temperature, and magnetic field. In Fig. 4 we plot the differential transmission at a positive delay corresponding to the maximum amplitude

of the negative $\Delta T/T$ (maximum enhanced absorption). For the 250 K data, presented in Fig. 4(a), $|\Delta T/T|$ increases as the power of the pump pulse increases consistent with our interpretation of an enhanced absorption due to indirect (non- \vec{k} conserving) processes involving scattering with the carriers created by the pump pulse. As the number of the photo-created carriers increases with the power of the pump pulse it is natural that the indirect absorption also increases.

At 250 K an applied magnetic field has little influence since the data taken at different magnetic fields are almost identical (as expected from the data presented in Fig. 1 which were taken at the maximum power). $|\Delta T/T|$ measured at lower temperatures can be seen in Figs. 4(b) and 4(c). It is clear that with decreasing temperature the magnetic field has an increased influence on the pump-pulse power dependence of $|\Delta T/T|$. For the lowest temperature of 18 K the signal at $B=6$ T is almost as twice as large as at 0 T. The change in the amplitude of the negative $|\Delta T/T|$ with a magnetic field can be explained using a simple rate-equation model where we consider pumping a level for 50 fs (duration of the pulse) and then escaping from this level with a 70 fs escape time (0 T decay time) and 110 fs (6 T decay time), which is presented in Fig. 4(d). As the negative value of $|\Delta T/T|$ is related to the number of carriers at an energy near the energy of the probe pulse it is strongly dependent on their escape time. The role of temperature can be understood as follows; with increasing lattice temperature the elastic electron-phonon scattering broadens the Landau levels and therefore suppresses the quenching of the Auger scattering. One should note that this is true even if the carrier temperature is much higher than the lattice temperature. For example, at a temperature of 50 K the thermal energy ($k_B T$) is comparable to the Landau-level separation.

IV. CONCLUSION

A pump-probe technique has been used to probe the carrier dynamics in multilayer graphene. We find that the hot-carrier relaxation is slowed in the presence of a magnetic field. This is interpreted as a reduction in electron-electron (Auger) scattering due to the unusual Landau quantization of Dirac fermions in graphene as well as a proof of the importance of the electron-electron scattering compared to the electron-phonon scattering in all the phases of the carrier relaxation and thermalization. Our measurements, which probe Landau levels with a high index ($n \approx 100$), suggest that for lower Landau levels, Auger processes may be completely suppressed. This makes graphene a promising system for the implementation of the long ago proposed³ tunable far-infrared Landau-level laser.

ACKNOWLEDGMENTS

This work has been supported by ANR under Contract No. PNANO-019-06, RTRA under Contract No. DISPOGRAPH FCSN-2008-09P, and CNRS under Contract No. PICS-4340. Two of us (P.P. and P.K.) are financially supported by the EU under FP7, Contracts No. 221249 “SESAM” and No. 221515 “MOCNA,” respectively.

*paulina.plochocka@grenoble.cnrs.fr

- ¹L. Rota, P. Lugli, T. Elsaesser, and J. Shah, *Phys. Rev. B* **47**, 4226 (1993).
- ²M. Potemski, R. Stepniewski, J. C. Maan, G. Martinez, P. Wyder, and B. Etienne, *Phys. Rev. Lett.* **66**, 2239 (1991).
- ³H. Aoki, *Appl. Phys. Lett.* **48**, 559 (1986).
- ⁴E. Gornik, *J. Magn. Magn. Mater.* **11**, 39 (1979).
- ⁵K. Ikushima, H. Sakuma, S. Komiyama, and K. Hirakawa, *Phys. Rev. Lett.* **93**, 146804 (2004).
- ⁶K. S. Novoselov, A. K. Geim, S. V. Morozow, D. Jiang, M. I. Katsnelson, I. V. Grigorieva, S. V. Dubonos, and A. A. Firsov, *Nature (London)* **438**, 197 (2005).
- ⁷Y. Zhang, Y.-W. Tan, H. L. Stormer, and P. Kim, *Nature (London)* **438**, 201 (2005).
- ⁸K. S. Novoselov, E. McCann, S. V. Morozow, V. I. Fal'ko, M. I. Katsnelson, D. Jiang, F. Schedin, and A. K. Geim, *Nat. Phys.* **2**, 177 (2006).
- ⁹A. H. Castro Neto, F. Guinea, N. M. R. Peres, K. S. Novoselov, and A. K. Geim, *Rev. Mod. Phys.* **81**, 109 (2009).
- ¹⁰T. Morimoto, Y. Hatsugai, and H. Aoki, *Phys. Rev. B* **78**, 073406 (2008).
- ¹¹J. M. Dawlaty, S. Shivaraman, M. Chandrashekar, F. Rana, and M. G. Spencer, *Appl. Phys. Lett.* **92**, 042116 (2008).
- ¹²D. Sun, Z. K. Wu, C. Divin, X. Li, C. Berger, W. A. de Heer, P. N. First, and T. B. Norris, *Phys. Rev. Lett.* **101**, 157402 (2008).
- ¹³R. W. Newson, J. Dean, B. Schmidt, and H. M. van Driel, *Opt. Express* **17**, 2326 (2009).
- ¹⁴P. A. George, J. Strait, J. Dawlaty, S. Shivaraman, M. Chandrashekar, F. Rana, and G. Spencer, *Nano Lett.* **8**, 4248 (2008).
- ¹⁵C. Berger, Z. Song, T. Li, X. Li, A. Y. Ogbazghi, R. Feng, Z. Dai, A. N. Marchenko, E. H. Conrad, and P. N. First, *J. Phys. Chem. B* **108**, 19912 (2004).
- ¹⁶C. Berger, Z. Song, T. Li, X. Li, X. Wu, N. Brown, C. Naud, D. Mayou, A. N. Marchenko, and E. H. Conrad, *Science* **312**, 1191 (2006).
- ¹⁷M. L. Sadowski, G. Martinez, M. Potemski, C. Berger, and W. A. de Heer, *Phys. Rev. Lett.* **97**, 266405 (2006).
- ¹⁸M. L. Sadowski, G. Martinez, M. Potemski, C. Berger, and W. A. de Heer, *Solid State Commun.* **143**, 123 (2007).
- ¹⁹C. Faugeras, A. Nerrière, M. Potemski, A. Mahmood, E. Dujardin, C. Berger, and W. A. de Heer, *Appl. Phys. Lett.* **92**, 011914 (2008).
- ²⁰A. E. Ruckenstein and S. Schmitt-Rink, *Phys. Rev. B* **35**, 7551 (1987).
- ²¹Z. Q. Li, E. A. Henriksen, Z. Jiang, Z. Hao, M. C. Martin, P. Kim, H. L. Stormer, and D. N. Basov, *Nat. Phys.* **4**, 532 (2008).
- ²²M. Breusing, C. Ropers, and T. Elsaesser, *Phys. Rev. Lett.* **102**, 086809 (2009).
- ²³T. V. Shahbazyan, N. A. Fromer, and D. S. Chemla, *Int. J. Mod. Phys. B* **18**, 3847 (2004).
- ²⁴E. Tsitsishvili and Y. Levinson, *Phys. Rev. B* **56**, 6921 (1997).
- ²⁵S. Kuroda and S. Komiyama, *Int. J. Infrared Millim. waves* **12**, 783 (1991).
- ²⁶M. Orlita, C. Faugeras, P. Plochocka, P. Neugebauer, G. Martinez, D. K. Maude, A.-L. Barra, M. Sprinkle, C. Berger, W. A. de Heer, and M. Potemski, *Phys. Rev. Lett.* **101**, 267601 (2008).